

---



**RASTAS  
SPEAR**

---

*Radiation-**S**hapes-**T**hermal Protection Investigations  
for High **S**peed **E**arth **R**e-entry*

**Final Report**

**RASTAS-Astrium ST-FR-01**

*Ed.1 - 20 Apr 2013*

Page 1/36

**Nature of document: Final Report**

**Author : O. Chazot (VKI), C. Laux (CNRS), G. Vekinis (Demokritos), E. Trifoni (CIRA), Z. Skorupka (IoA), B. Chanetz (ONERA), J. Vos (CFS), M. Gritsevich (Lomonosov Moscow State University), O. Sladek (Kybertec), J.-M. Bouilly, A. Bourgoing & A. Pisseloup (Astrium ST)**



# Summary

<b>ABBREVIATIONS .....</b>	<b>3</b>
<b>1. INTRODUCTION .....</b>	<b>5</b>
<b>2. SCOPE .....</b>	<b>6</b>
2.1 PROJECT OVERVIEW.....	6
2.2 MOTIVATION FOR RASTAS SPEAR PROJECT .....	6
2.3 TECHNICAL ORGANISATION.....	7
<b>3. WP1: REVIEW OF SYSTEM REQUIREMENTS .....</b>	<b>8</b>
3.1 WP1.1 – ATMOSPHERE MODELLING .....	8
3.2 WP1.2 – TRAJECTORIES.....	8
3.3 WP1.3 – AERODYNAMICS AND AEROTHERMODYNAMICS.....	9
3.4 WP 1.4 – VEHICLE DESIGN.....	10
<b>4. WP2 : GROUND FACILITIES FOR HIGH-SPEED RE-ENTRY TESTING.....</b>	<b>11</b>
<b>5. WP3: KEY TECHNOLOGIES FOR HIGH SPEED ENTRY .....</b>	<b>13</b>
5.1 TPS AND JOINTS .....	13
5.2 ARCJET TESTS .....	14
5.3 BREADBOARD MANUFACTURING.....	15
5.4 CRUSHABLE STRUCTURE .....	16
<b>6. WP 4: ABLATION - FIGHT MECHANICS COUPLING ASSESSMENT .....</b>	<b>21</b>
6.1 IMPLEMENTATION AND ASSESSMENT OF COUPLED TOOL.....	21
6.2 ENGINEERING MODELLING CORRECTION BY CFD (WP 4.3) .....	23
6.3 EXPERIMENTAL ASSESSMENT OF RADIATING SPECIES AROUND ABLATING MATERIALS (WP4.4 - CNRS).....	25
<b>7. WP5: GAS-SURFACE INTERACTION MODELLING.....</b>	<b>26</b>
7.1 AN EXPERIMENT TO SIMULATE THE COUPLING BETWEEN ABLATION AND PYROLYSIS PRODUCTS .....	26
7.2 EXPERIMENTAL RESULTS .....	28
7.3 GAS-SURFACE INTERACTION MODELLING .....	31
7.4 CFD MODELLING (WP5.3 - CFS) .....	32
7.5 SUMMARY STATUS FOR WP5.....	33
<b>8. WP6: MANAGEMENT, DISSEMINATION AND EXPLOITATION .....</b>	<b>34</b>
<b>9. CONCLUSION .....</b>	<b>36</b>



## ABBREVIATIONS

BC	Back-Cover
BS	Back Shell
CAD	Computer Aided Design
CFRP	Carbon Fiber Reinforced Polymer
COG	Centre of Gravity
ERC	Earth Return Capsule
EVD	Entry Vehicle Demonstrator
EVE	European Venus Exploration
FS	Front Shield
HS	Heat Shield
IF	Interface
MSR	Mars Sample Return
NL	Norcoat Liege
SEM	Scanning Electron Microscope
TP / TPS	Thermal Protection / Thermal Protection System
TRL	Technology Readiness Level
TRR	Test Readiness Review



## REFERENCES

- [1] [www.rastas-spear.eu](http://www.rastas-spear.eu)
- [2] J-M. Bouilly et al, RASTAS SPEAR: Radiation-Shapes-Thermal Protection Investigations for High Speed Earth Re-entry, 9th International Planetary Probe Workshop IPPW9, June 18 - 22, 2012, Toulouse
- [3] J-M. Bouilly et al, RASTAS SPEAR: Radiation-Shapes-Thermal Protection Investigations for High Speed Earth Re-entry, 8th International Planetary Probe Workshop IPPW8, June 18 - 22, 2011, Portsmouth
- [4] Neumann R.D., Experimental Methods for Hypersonics: Capabilities and Limitations, 2nd Joint Europe-US Short Course on Hypersonic: GAMNI-SMAI and Uni. Of Texas at Austin, USAF Academy, Colorado springs, CO 80840, January 1989.
- [5] Fay, J.A., Riddell, F.R., Theory of stagnation point heat transfer in dissociated air, Journal of Aeronautical Sciences, Vol. 25, No. 2, February 1958, p. 73-85.
- [6] Lees L., Laminar heat transfer over blunt-nosed bodies at hypersonic flight speed, Jet Propulsion, Vol. 26, April 1956, pp. 259-269.
- [7] Kolesnikov A.F., Condition of simulation of Stagnation Point heat transfer from High enthalpy flow, Fluid Dynamics, Plenum, (tr. From Russian), 1993, v.28, No. 1, pp 131-137.
- [8] Kolesnikov, A. Extrapolation from high enthalpy tests to flight based on the concept of LHTS. Belgium. RTO-VKI Special course. Measurement Techniques for High Enthalpy and Plasma Flows, October 1999.
- [9] Chazot O., R. Régnier and A. Garcia Muñoz, Simulation Methodology in Plasmatron Facility and Hypersonic Wind Tunnels, 12th International Conference on Method of Aerophysical Research, Akademgorodok, Novosibirsk, Russia, June 28 – July 4, 2004.
- [10] Chanetz B., Vos J., Bourgoing A., Gas-Surface Interactions modeling, 7th European Workshop on TPS & Hot Structures - Noordwijk (NL), 2013, April 8-10
- [11] Bourgoing A., DeChampvallins N, High Speed Entry Ablation-Flight Mechanics Coupling Effects, 7th European Workshop on TPS & Hot Structures - Noordwijk (NL), 2013, April 8-10
- [12] Vekinis G., Overview of the TPS Activities within the RASTAS SPEAR Project, 7th European Workshop on TPS & Hot Structures - Noordwijk (NL), 2013, April 8-10
- [13] Laux C., Mc Donald M., Characterization of a 50 kW Inductively Coupled Plasma Torch for use in Testing of Ablative Materials, 7th European Workshop on TPS & Hot Structures - Noordwijk (NL), 2013, April 8-10



## 1. INTRODUCTION

An important step for Space Exploration activities and for a more accurate knowledge of the Earth, universe and environment is to develop the capability to send vehicles into space, which collect and return to Earth samples from solar system bodies. To return these samples, any mission will end by high-speed re-entry in the Earth's atmosphere. This requires strong technological bases and a good understanding of the environment encountered during the Earth re-entry.

Investment in high speed re-entry technology development is thus appropriate today to enable future Exploration missions such as Mars Sample Return. Rastas Spear project started in September 2010, with the main objective to increase Europe's knowledge in high speed re-entry vehicle technology to allow for planetary exploration missions in the coming decades.

The research leading to these results has received funding from the European Union Seventh Framework Programme (FP7/2007-2013) under grant agreement n° 241992.

The project's main objective can be sub-divided into sub-objectives as follows:

- **OBJ1:** To better understand phenomena during high speed re-entry, enabling more precise Capsule sizing and reduced margins,
- **OBJ2:** To identify the ground facility needs for simulation,
- **OBJ3:** To master heat shield manufacturing techniques and demonstrate heat shield capabilities.
- **OBJ4:** To master damping at ground impact and flight mechanics and thus ensure a safe return of the samples.

This study is carried out by a consortium of 10 European companies and institutes: VKI (B), Kybertec (Cz), Demokritos (Gr), IoA (PI), CIRA (I), CFS (CH), MSU (Ru), CNRS and ONERA (F), and coordinated by Astrium (F).

The aim of this paper is to present the organisation, objectives and main actions proposed in the RASTAS SPEAR project, to enlarge the basic capabilities on some specific topics such as:

- Aeroshape stability
- High speed aerothermal environment
- Sub-system / equipment : Thermal protection, Crushable material



## 2. SCOPE

### 2.1 PROJECT OVERVIEW

This project received funding from the European Union Seventh Framework Programme (FP7/2007-2013) under grant agreement n° 241992. It was selected as part of the FP7 second call, in the following topics:

- Activity 9.2 – strengthening of space foundations / research to support space science exploration
- SPA.2009.2.1.01 Space Exploration

Rastas Spear started in September 2010 and was completed in April 2013.

The total budget was 2.3 M€, including a 1.6 M€ grant from the European Commission.

10 partners from 8 European Countries (see Table 2-1) were part of the team and Astrium SAS was the coordinator.

More information can be found on the project website at [www.rastas-spear.eu](http://www.rastas-spear.eu)

Partner	Country
ASTRIUM Space Transportation SAS	France
CIRA : Centro Italiano Ricerche Aerospaziali	Italy
CFS Engineering	Switzerland
NCSR Demokritos	Greece
CNRS	France
IoA : Institute of Aviation	Poland
KYBERTEC	Czech Republic
MSU : Lomonosov Moscow State University	Russia
ONERA : Office National d'Etudes et de Recherches Aéropatiales	France
VKI : Von Karman Institute for Fluid Dynamics	Belgium

Table 2-1 : Partners involved in Rastas Spear project

### 2.2 MOTIVATION FOR RASTAS SPEAR PROJECT

As mentioned in the introduction, Sample Return Missions are considered as an important step for Solar System Exploration. Some essential technical aspects are reminded below:

- After collecting samples, any return mission will end by high-speed re-entry in the Earth's atmosphere.
- This requires strong technological bases and a good understanding of the environment encountered during the Earth re-entry.

It was therefore deemed paramount to invest today in high speed re-entry technology development, in order to increase Europe's knowledge in such re-entry vehicle technology and hence pave the way for future planetary exploration missions in the coming decades (Mars Sample Return, Marco Polo...)

Spinoff is also considered for other potential applications with high speed atmospheric entry (ISS return (ARV), Venus Exploration (EVE-VEP)).

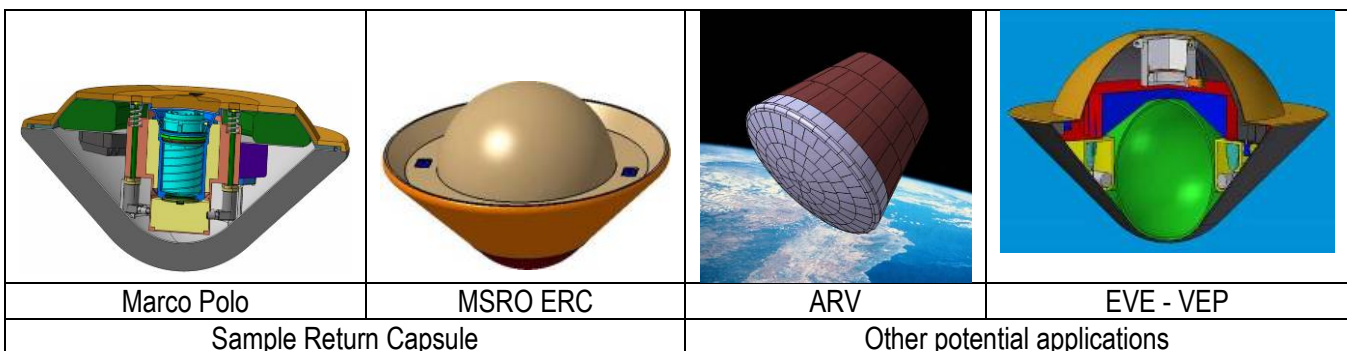


Figure 2-1: Future European atmospheric entry missions with high speed entry



## 2.3 TECHNICAL ORGANISATION

In order to achieve the project goal, the main objective is derived in sub-objectives as follows and adequately split in 6 Work Packages (see Figure 2-2) that address these different sub-objectives:

- OBJ1 (WP1, WP2, WP4 + WP5): To better understand phenomena during high speed re-entry enabling more precise Capsule sizing and reduced margins.
- OBJ2 (WP2) :To identify the ground facility needs for simulation
- OBJ3 (WP3): To master heat shield manufacturing techniques and demonstrate heat shield capabilities.
- OBJ4 (WP3+WP4) : To master damping at ground impact and flight mechanics and thus ensure a safe return of the samples

WP 6 consists of two main tasks for the whole duration of the project: the project management, and the coordination of internal and external communication.

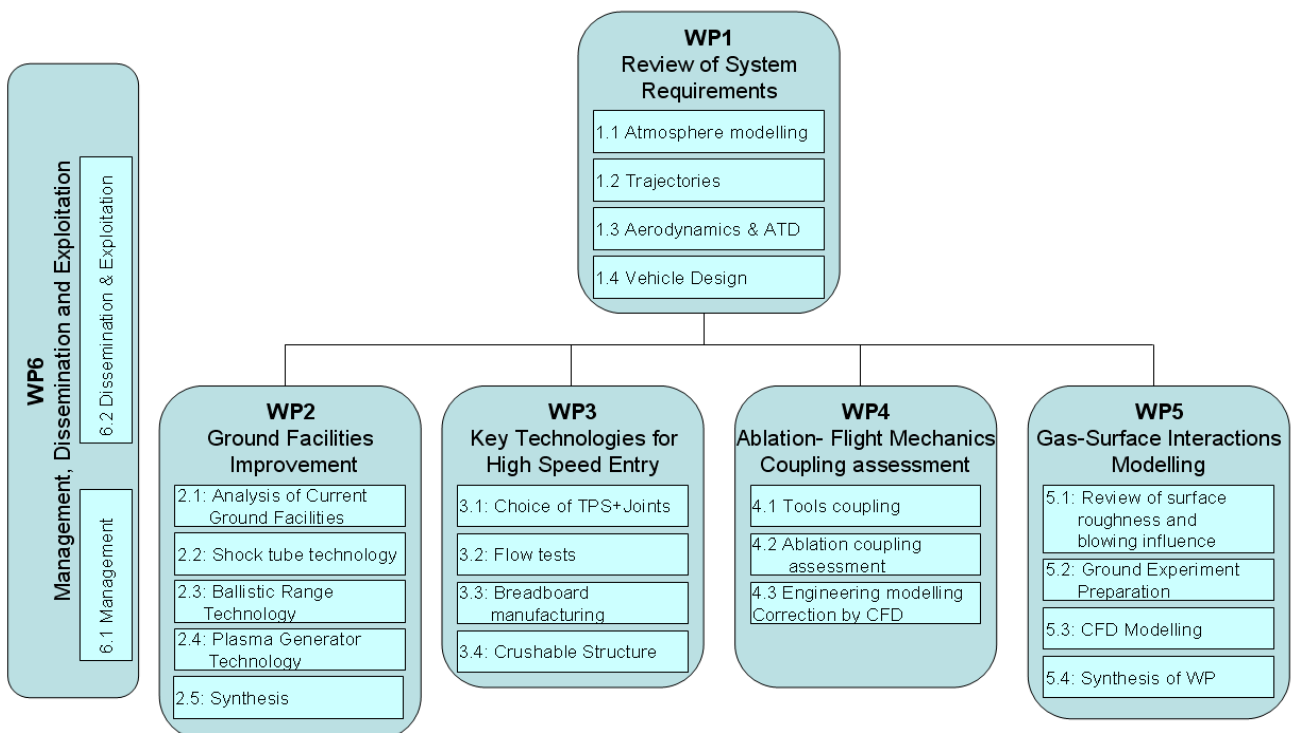


Figure 2-2: Project WBS

Table 2-2 below identifies the contributors and leader of each Work Package.

Work Packages titles	WP Participants and <u>Leader</u>
WP1 Review of System Requirements	AST, CNRS
WP2 Ground Facilities Improvement	AST, CIRA, CNRS, VKI
WP3 Key Technologies for High Speed Entry Mastering	AST-F, CIRA, DEMOKRITOS, IOA
WP4 Ablation-Flight mechanics coupling assessment	AST, CIRA, CNRS
WP5 Gas-Surface interactions modelling	AST, CFS, MSU, ONERA
WP6 Synthesis, Management & Coordination	AST + KYBERTEC, + WP leaders

Table 2-2: Work packages: titles, participants and leaders,



### 3. WP1: REVIEW OF SYSTEM REQUIREMENTS

This WP deals with the definition of general system requirements for high-speed entry capsules and its main objective is thus to provide with general inputs for any other WP of the project. Among future exploration missions, capsules can experience high-speed entries when samples from any asteroids or planets (Mars Sample Return mission, Stardust, Japanese Hayabusa for instance) are brought back to Earth for instance or when they enter into any solar system Giant planets (Jupiter, Saturn, Uranus, Neptune) for atmosphere science investigation (US Galileo mission for instance).

This WP is divided into four sub-tasks presented hereafter:

#### 3.1 WP1.1 – ATMOSPHERE MODELLING

WP1.1 is dedicated to the definition of atmosphere data that are necessary to be identified for any entry vehicle. For Earth or Mars atmospheres, data are available and largely documented (CIRA 88, GRAM, Mars-GRAM, EMCD). For any other planets, it is worth reviewing the atmosphere models available on Venus ( $V_e \sim 11.6$  km/s), Saturn, Jupiter, Uranus and Neptune ( $V_e \sim 30-60$  km/s). This is particularly important for WP2 task where ground facilities will be identified with respect to the gas composition to be tested.

A Thermochemical model (kinetic model + thermal model) has thus been established as reference, with identification of all possible species and chemical reactions. It has been decided to focus on Atmosphere compositions for Earth and Venus, as shown in Table 3-1: Thermochemical atmosphere models available for the project below.

EARTH	VENUS
complete model based on N <sub>2</sub> , O <sub>2</sub> and Ar	model based on CO <sub>2</sub> and N <sub>2</sub> mixture
simplified model based only on N <sub>2</sub> and O <sub>2</sub>	

Table 3-1: Thermochemical atmosphere models available for the project

#### 3.2 WP1.2 – TRAJECTORIES

WP1.2 is dedicated to identification of generic aeroshapes with respect to candidate exploration missions, with focused attention towards Earth entry. Trajectories have been computed including usual design criteria and flight domain has been determined with classical constraints on several parameters (max heat flux, max heat load, max g-load,...) Particular attention however will be paid on sample return to Earth missions.

The main features of the selected shape are summarized on Figure 3-1: ERC Shape, while Figure 3-2 shows the typical evolutions of some essential aerothermodynamic parameters.



Diameter  $D = 1100$  mm  
45° half cone angle (  
Nose radius  $R_n = 275$  mm ( $R_n / D = 0.25$ )  
Shoulder radius  $R_s = 27.5$  mm ( $R_s / D = 0.025$ )  
G-load requirement 2000g on the sample canister at impact

Figure 3-1: ERC Shape



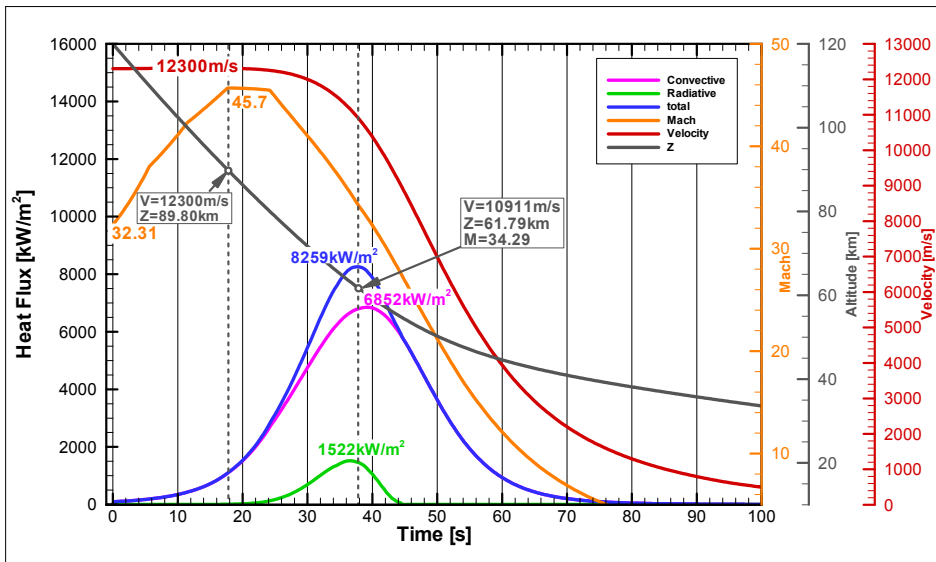
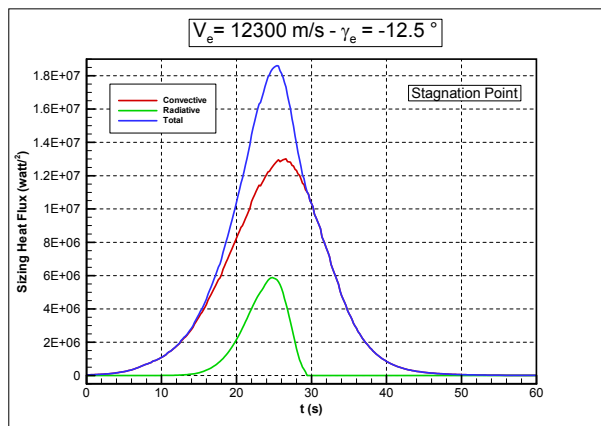


Figure 3-2: Heat Flux, Mach, Z, V vs. time for the FPAe=-8.5deg @120km trajectory

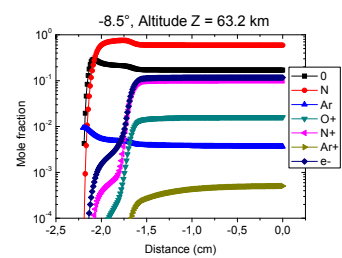
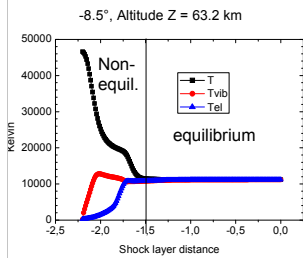
### 3.3 WP1.3 – AERODYNAMICS AND AEROTHERMODYNAMICS

WP1.3 deals with the aerodynamics and aerothermodynamics characterization of selected aeroshapes. Most of the data are derived from existing database available at Astrium-ST. Aerodynamics results are based on Newton preliminary analyses.

Aerothermal environment has been determined using engineering methods for convective heating while radiative heating is based on shock-layer radiation computations with the radiation code SPECAIR of CNRS/Laboratoire EM2C.



#### Contributions to the radiative flux of the equilibrium and nonequilibrium zones



- Nonequilibrium zone produces less than 19% of the radiative flux
- Less than 8% between -2.2 and -1.7 cm.



Figure 3-3: Determination of convective and radiative environment



### 3.4 WP 1.4 – VEHICLE DESIGN

WP1.4 aimed at a preliminary design of the generic capsule (see Figure 3-4), including the determination of TPS thickness, in order to define the Mass Centering and Inertia (MCI) for the given architecture. Preliminary requirements related to TPS for other WP have also been established thanks to 1 or 2D thermal models of the capsule: surface recession, mass loss, temperature evolution, gas flow rate,...

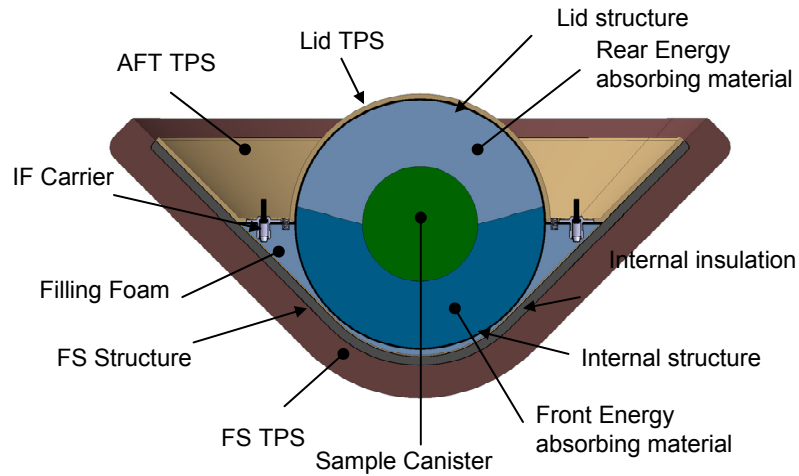


Figure 3-4: preliminary ERC design



## 4. WP2 : GROUND FACILITIES FOR HIGH-SPEED RE-ENTRY TESTING

The severe aerothermodynamics environment encountered by a space vehicle during a planetary re-entry has to be reproduced at best in ground-based facilities to allow a precise understanding of the flow properties around the vehicle and an accurate evaluation of the Thermal Protection System (TPS) performances. In such situation dedicated ground testing capabilities appear as a strong requirement for TPS design. Firstly, they represent a first convenient step in the testing procedure at reduced cost compared with the launch of a mission. Secondly, the ground tests allow a better control of the environment and the measurement techniques to investigate TPS properties and to develop qualification tests. However, as well known, a complete experimental simulation of hypersonic conditions on a model, in a ground test facility, is almost impossible to achieve or at best impractical in a laboratory [4]. Nevertheless on one hand methodologies have been elaborated with specific high-enthalpy facilities to duplicate the features of the post shock environment for high-speed entry [5, 6]. On the other hand plasma wind tunnels have been developed to address the aerothermodynamic testing of TPS for critical points of space vehicles in typical re-entry conditions [7-9]. Those plasma facilities provide testing conditions with relevant heat-flux level but where the radiation heating remains a small amount of the total heat-flux.

However space exploration program requires the development of space vehicles able to manage a safety return through the Earth atmosphere. Mars sample return which is the main focus of the RASTAS SPEAR project will lead to very severe conditions. Those high speed re-entry conditions are an issue for the current ground testing simulation due to their important radiation features and the coupling phenomena they involved. In this context a review on the existing ground based facilities for high speed re-entry and TPS qualifications has been completed. In one hand it appears that only few ground based facilities are able to cover the typical super orbital re-entry conditions of the RASTAS SPEAR project. On top of that, considering hyper-velocities wind tunnels none of these facilities are located in Europe. They represent an essential tool to study the mission and investigate the re-entry environment that will need to be simulated in the frame of the TPS design. In the other hand the European plasma wind tunnels dedicated to the qualification of TPS offer suitable testing conditions regarding the typical heat-flux levels along the high speed re-entry been considered.

In parallel to the worldwide facility review the measurement techniques for flow characterization have been listed for each of the high enthalpy and plasma wind tunnels. It appears that European facilities are generally well equipped with specific instruments that allow to cover a large spectrum for flow diagnostics.

In response to the lack of testing capabilities for super-orbital flight in Europe a preliminary design of an expansion tube has been investigated. This facility aims to offer a testing envelope for high speed re-entry conditions corresponding to the Rastas Spear project. A series of 1D numerical simulations were performed in order to achieve the optimal configuration leading to the target free stream conditions. All the elements of the expansion tube, from the driver to the test section have been calculated based on the X facilities operating in Australia.

Finally a test strategy combining the two types of facilities has been discussed. It would follow the use of high enthalpy facilities and plasma wind tunnels independently to determine specific radiation and gas surface interaction modelling thanks to dedicated measurement and suitable physical analysis of the phenomena occurring during the tests. The testing methodology could be represented as in Figure 4-1. The models obtained from the database, generated with the two type of testing facility, are used in CFD tools. The coupling phenomena are realized through the numerical computations that serve as input to the thermo-structural analysis for the final TPS sizing.



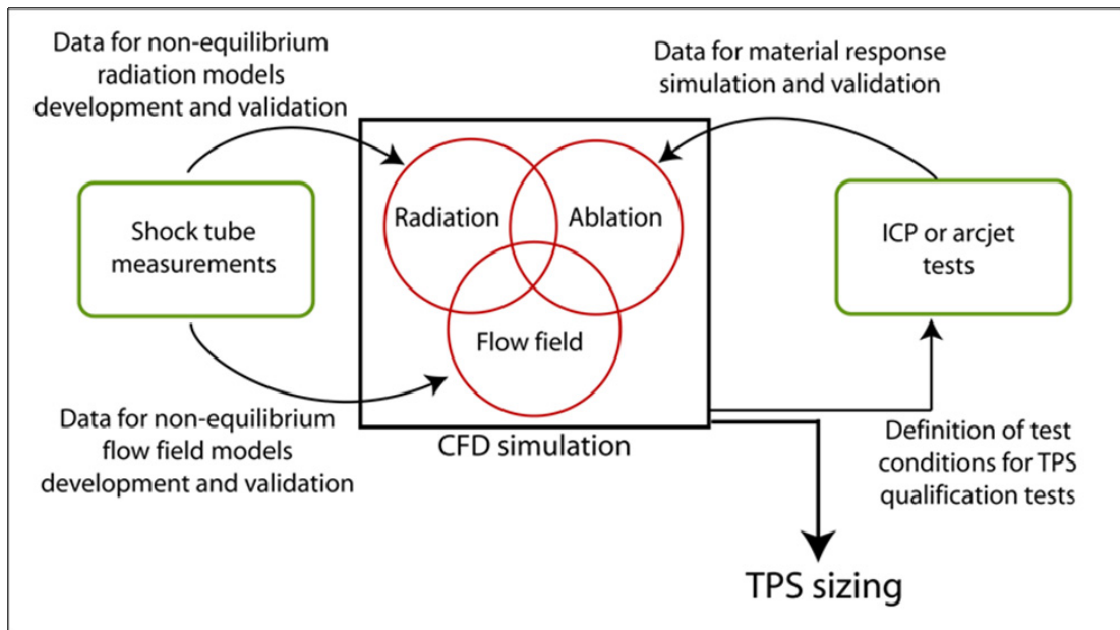


Figure 4-1: Testing methodology for high speed re-entry TPS sizing



## 5. WP3: KEY TECHNOLOGIES FOR HIGH SPEED ENTRY

This activity about technologies that need to be developed for the ERC was led by NCSR Demokritos. Specifically, the main objectives of WP3 were to investigate and develop new and innovative methods, materials and systems for joining the ablative blocks together and to the substructure, to produce a complete Thermal Protection System (TPS) for sample-return missions. Another topic was also considered, related to the crushable material which would absorb the impact forces during the probe's hard landing on Earth.

### 5.1 TPS AND JOINTS

#### General approach

The TPS can be sorted in 3 main components: the thermal protection material itself, the joint material to be positioned between different tiles or blocks, and the bonding process to fix the TP material on the underlying substructure.

Appropriate thermal protection materials are available: based on outcomes from WP1, the low density carbon-phenolic ablator "ASTERM" has been selected as baseline for the project. But the gap/seam materials are still to identify, which is one main goal of this WP3 activity [12], with the main following sub-tasks:

- Elaboration of a relevant set of criteria: Among the various considerations, a comparable but slightly higher recession than that of the surrounding material is searched. Another important consideration is the interest for relatively simple and cheap processing methods.
- Selection and elementary testing of appropriate joint materials
- Plasma testing of samples with Asterm + most promising joint materials
- Manufacturing of a technological breadboard

These different topics are summarized in the following sections.

#### Screening and Trade-off for gap-seam material

Based on above-mentioned requirements, screening tests were applied to various commercially available adhesives : evaluation of their out-gassing, volatility, low temperature (-196°C) mechanical behaviour, ease of handling, cost, ease of bonding to a fibrous substrate, curing conditions (time, humidity, air effect), ablation behaviour under propane gas flame.

Investigations were performed on 9 adhesives, among which CV1142 and another 2 adhesives (Mega Grey ("MG") and Mega Copper ("MCu")) passed all thresholds and were selected for bond testing (tensile, shear and bending) in following step.

- CV1142 (made by NUSIL) used on Beagle 2 was chosen as reference material for comparative bond testing in this project
- MG and MCu are both inexpensive, commercial HT gasket silicones in the UK and USA. These RTV (room temperature vulcanizing) silicones cure into a silicone rubber that maintains long term durability and flexibility to make formed-in-place gaskets. They are all used for high temperature gasketing applications. According to their technical specifications, they have similar composition to CV1142

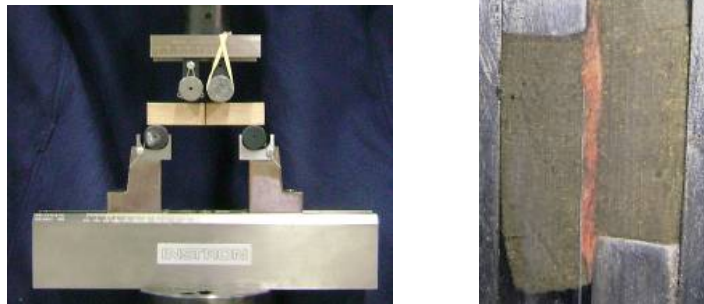


Figure 5-1: bending and shear testing



Mechanical testing was carried out under direct shear, as mentioned above. It was found that in all cases, the adhesive joint is stronger than the ASTERM material: fracture occurred through the ASTERM in all cases.

The partial conclusion after mechanical testings is that MG and MCu indeed both offer a potentially viable alternative to CV1142, at least as far as their bonding and mechanical properties are concerned. Their curing behaviour and non-use of primer appears to also offer advantages for manufacturability of a shield. These adhesives were therefore selected for the next phase consisting of Plasma-jet tests.

## 5.2 ARCJET TESTS

### Manufacturing of samples for plasma tests

After selection of appropriate silicone glues as above mentioned, this task consisted of two main parts:

- Actual production of samples to be tested in plasma test campaigns planned in WP3.2.
- Expertise of the samples after they have been tested (described in following section).

A first series of samples was produced for testing at Scirocco. Their geometry has been identified by CIRA and Astrium as a flat-top cone of plasma-facing diameter about 65mm. The samples are first machined from ASTERM and then cut and re-joined using a total of 4 joints each with a different adhesive (see Figure 5-2). CV1142 is used as reference and MG and MCu are used alone or mixed with various quantities of powdered ASTERM.

After reorientation of the test campaign (see next section), a new batch of samples was produced, each with 4 different adhesive joints as before (see Figure 5-3). In order to fit with DLR L3K facility, sample dimension was smaller (diameter 50 mm) than those for Scirocco. In the meantime, it was also decided to include a new candidate in the panel of tested adhesives: ESP495, which is the product used for ExoMars heatshield.

### Arc Jet tests with different tiles accommodation

This task consisted of an experimental assessment of the identified concepts, with the aim to consolidate the selection of the best joint materials. Arc-jet testing was undertaken, as the most satisfactory simulation wrt actual flight conditions.

The initial rationale for the tests was the following:

- Performance of four plasma tests on the Scirocco facility of CIRA at moderate heat flux (5 MW/m<sup>2</sup>)
- Analysis of the results and selection of the two most promising gap/seam materials
- Performance of two tests at higher heat flux (15 MW/m<sup>2</sup>)

### Testing at Scirocco

A first test campaign took place at CIRA in October-November 2011 where two runs were performed. During this first campaign, two sample holders broke off.

Only the first test at 5 MW/m<sup>2</sup> had a sufficient duration of 12 sec to allow some expertise of the sample. However, it was damaged due to the breakage of the supporting graphite arm. One of the MCu adhesive joints survived intact and showed good behaviour. Figure 5-2 shows pictures of the sample before and after test.



Figure 5-2: ASTERM TPS before and after Scirocco arc jet test



After this test campaign, CIRA detected early 2012 a problem on Scirocco's power supply system leading to a long unavailability of the facility. The logic had thus to be totally reshuffled and it was decided in Autumn 2012 to shift the remaining tests to another arcjet test facility in Europe, at DLR, Köln, Germany.

### Test campaign at DLR L3K

A new test plan was established for testing on the L3K facility of DLR, with proposed test conditions already experienced in former studies.

- 15 tests in total were carried out on samples with various joints materials.
- 9 tests at 6.1 MW/m<sup>2</sup>, with different durations of 25 and 30 sec for comparison
- 6 tests at 13.6 MW/m<sup>2</sup>, also with different durations of 10 and 15 sec, finally reduced to 9 and 12 sec, after the first test had to be stopped after 14 sec due to excessive erosion.

As these tests were completed quite late in the study, very little time was remaining for the expertise of the samples. A pretty satisfactory analysis was however achieved, the main conclusions of which are summarized below:

- CV1142 and ESP495 display good erosion resistance at 6 MW/m<sup>2</sup> (see Figure 5-3).
- At 13.6 MW/m<sup>2</sup>, erosion becomes more important for these two adhesives, while it is unacceptable for the two other MCu and MG.

The interest of adding Asterm powder to the adhesive as reinforcement is demonstrated.

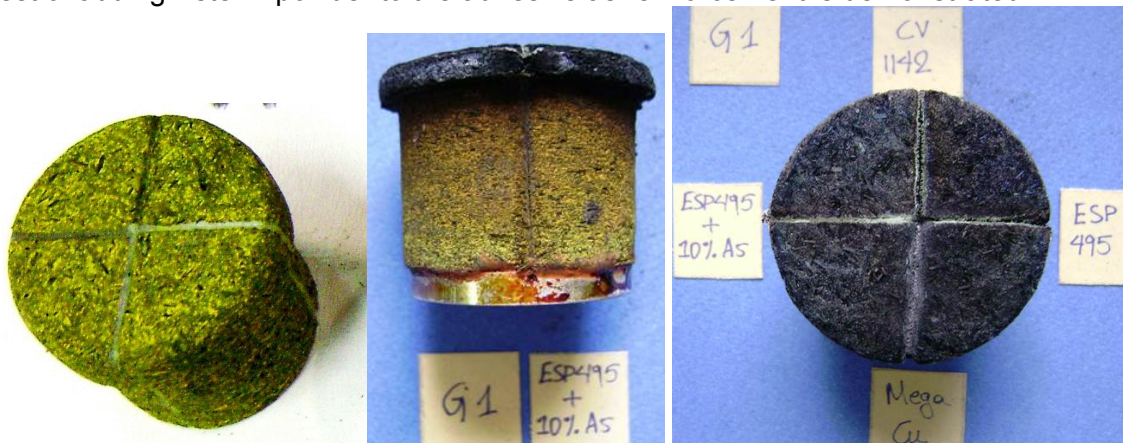


Figure 5-3: ASTERM TPS with joints, before and after arc jet test at 6 MW/m<sup>2</sup> on DLR L3K facility

### 5.3 BREADBOARD MANUFACTURING

This task consisted of the design and manufacturing of a technological breadboard representative of a TPS shield for a sample-return mission. The objective was to demonstrate the effective and efficient feasibility of the proposed TPS shield concept, with relevant geometry and dimensions, to be as representative as possible of the targeted application.

The Demonstrator Heat Shield was built in two stages. Design of the tiles on the shield was firstly completed (including FEM) and formed the basis of the dimensioning and manufacturing of the tiles. Considering the available amount of ASTERM material, a maximum diameter of about 90cm was proposed. This represents a reduction of about only 18% from the reference shape designed in WP1 (see Figure 3-4), which is considered fairly representative, as the overall shape and the total TPS thickness of 56 mm are applied.

In order to investigate a low cost approach, it was decided to manufacture this prototype following a predominantly manual process. Specifically, tiles of approximate dimensions are cut with the right angles on carpenter's circular saw which are then shaped by manual shaping with suitable sand paper against the truncated cone substrate and 3 special truncated cone rings at suitable positions. Once all the tiles (3 layers of 12 tiles each) are prepared, they are glued onto the substrate and joined between them, with bond and joints of about 1 to 1.5 mm thick max. In the next stage the totality of the 36 tiles bonded onto the substrate are "shaved" in one operation using a rotating "shaving tool" to the required thickness,



thereby ensuring exact radial symmetry of the whole structure. Finally, the nose piece is also shaped using a spherical arc tooling guide and then bonded onto the prepared cone. All these operations were described in a specific procedure established as preparatory work. As a precaution and to optimise the manufacturing method, it was decided to first develop the whole process using a simulating material (high density expanded polyurethane HDEPU) with which a complete demo was made. Once all the stages are completed and well-tuned, the actual DEMO breadboard was built using the ASTERM material, with an actual final diameter of 92.5cm.

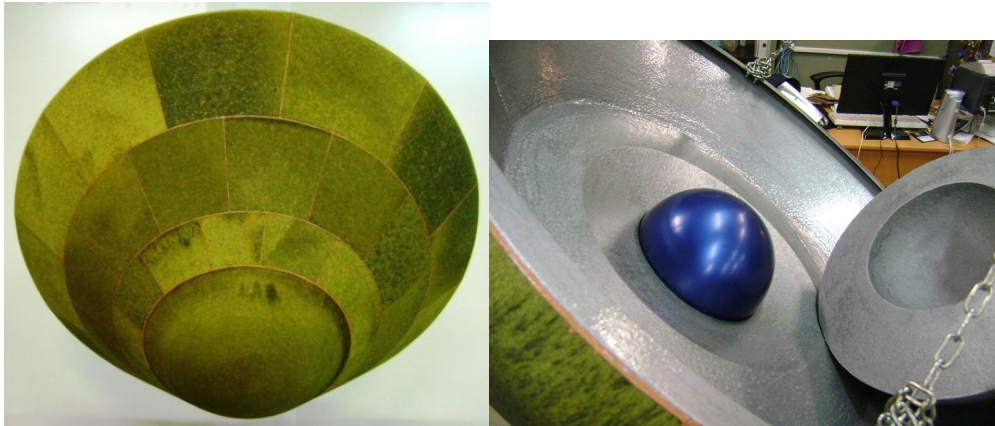


Figure 5-4: Demonstrator with ASTERM TPS; Crushable material insert and sample sphere

Capability for actual implementation of such a low cost manual process is relevant, as there is for sure potential for further improvement, using greater precision tooling. This might become an attractive alternative to usual methodology, provided current dimensional tolerances are relaxed to some extent

## 5.4 CRUSHABLE STRUCTURE

### General approach

This activity about crushable structures was managed by IoA Warsaw, with the following main objectives:

- Propose a suitable impact absorbing material for future application in sample-return re-entry vehicles.
- Provide numerical simulation, calculations and analysis, which will lead to right choice of crushable structure. Identify an appropriate mathematical model of the material behaviour to picture the phenomenon
- Select the final material and provide the method and material for assembly on demonstrator.

Figure 5-5 depicts the progressive approach initially planned for this activity. After procurement of candidate materials, a step by step selection was undertaken relying on three types of tests: static, low speed dynamic, crush test.

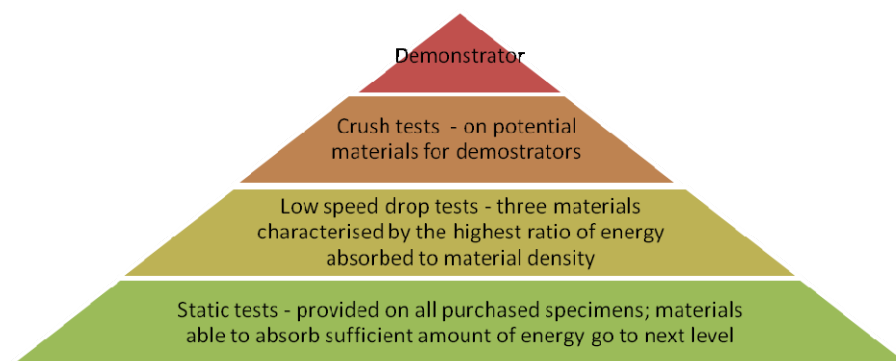


Figure 5-5: Step by step approach for crushable materials



**Material screening**

The activity started with investigations carried out about state of knowledge, technology readiness and commercial applications of this type of materials.

This prospective relied on a set of requirements established in WP1: lightweight material, good energy absorber during crush, quasi isotropic, thermally stable and insulator, compatible with vacuum, reproducible manufacturing process.

Figure 5-6 presents a few crushable materials resulting from the screening, covering various types of materials such as polymeric, metallic and brittle foams, as well as different ranges of density.

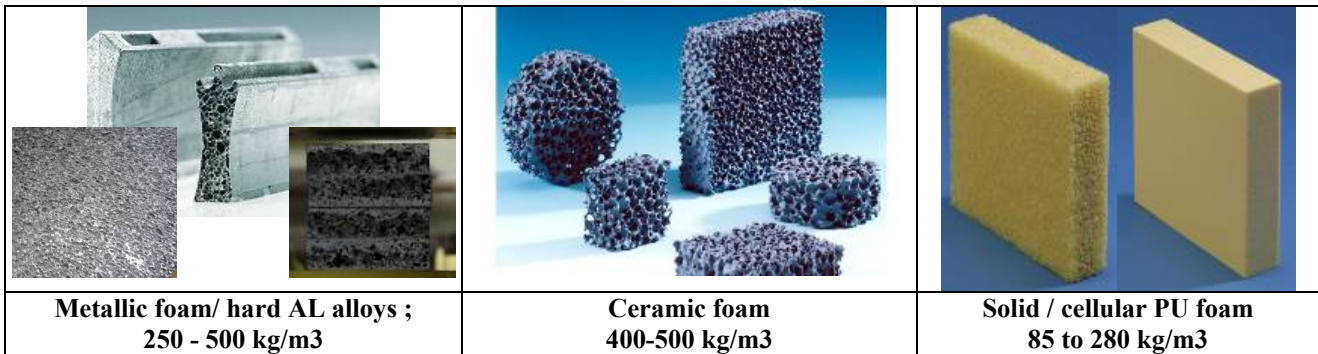


Figure 5-6: Typical crushable materials identified within the activity

**Static tests**

Based on the above-mentioned screening, a total of 20 different energy absorbing materials were tested. The shape of the tested specimens was finalised as cubes of side 100mm (see Figure 5-7). This series of quasi-static tests was performed on a 40 T hydraulic press available in Landing Gear department of IoA.

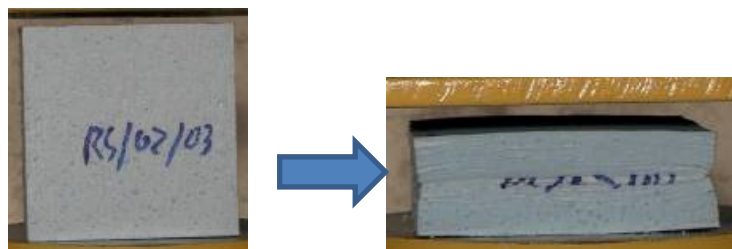


Figure 5-7: Typical material deformation during static test

These tests allowed determining the strength behaviour and capability for energy absorption for the considered materials. Comparative results in Figure 5-8 show that different behaviours are observed, making possible an optimised selection depending on required strength and deceleration capability.

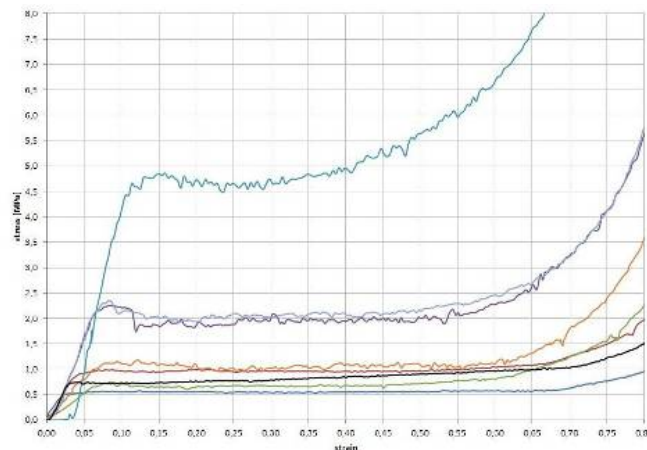


Figure 5-8: Comparative stress-strain characteristics determined for various materials



### Low speed dynamic tests

A few tests were actually performed following the approach initially defined, and using the 10T drop test machine available at IoA. However, it turned out that it was uneasy to get satisfactory measurements. It was then preferred to rely only on a 2-step approach based on static tests and high speed tests.

### High speed dynamic tests (samples)

During the first year of the project, a crash test stand had been designed and prepared. Preliminary tests and analysis showed problems with dissipating energy accumulated during acceleration phase. Additionally, projected (quoted) costs for the systems needed for this original design exceeded available resources.

A new test approach was therefore defined using a different technique: a horizontal pneumatic cannon. The cannon system was purchased after completion of the design that required further analyses. Development, assembly, calibration and implementation of most appropriate measurements was then successfully undertaken, though it turned out to be more tricky than anticipated. Following this important preparatory phase, tests using cannon with a high speed projectile (45 m/s) were carried out from April to July 2012.

Based on the results from the two previous test stages, those further tests were performed on eight most promising materials.

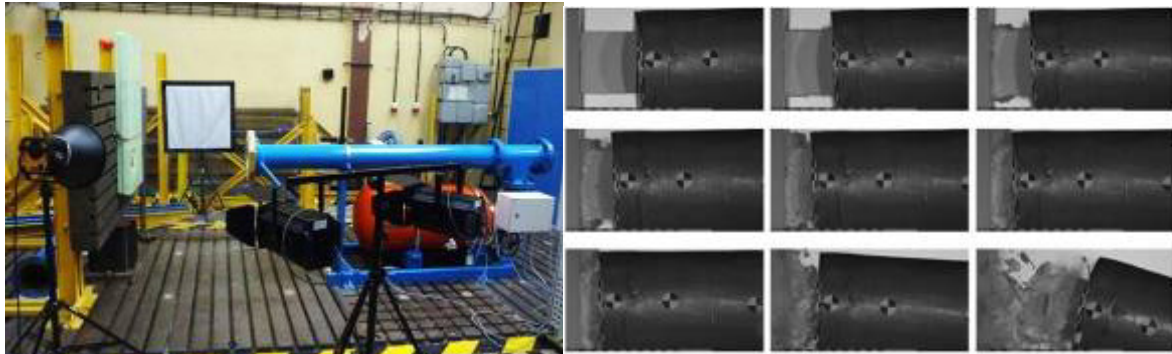


Figure 5-9: Air cannon and pictures from high speed camera during test

A numerical rebuilding of tests was then performed, using the LS-Dyna code, and taking into account as inputs material data obtained from static tests. As an example, Figure 5-10 shows a pretty good comparison obtained for the PU foam SR10 between the FEM model and the experiment data.

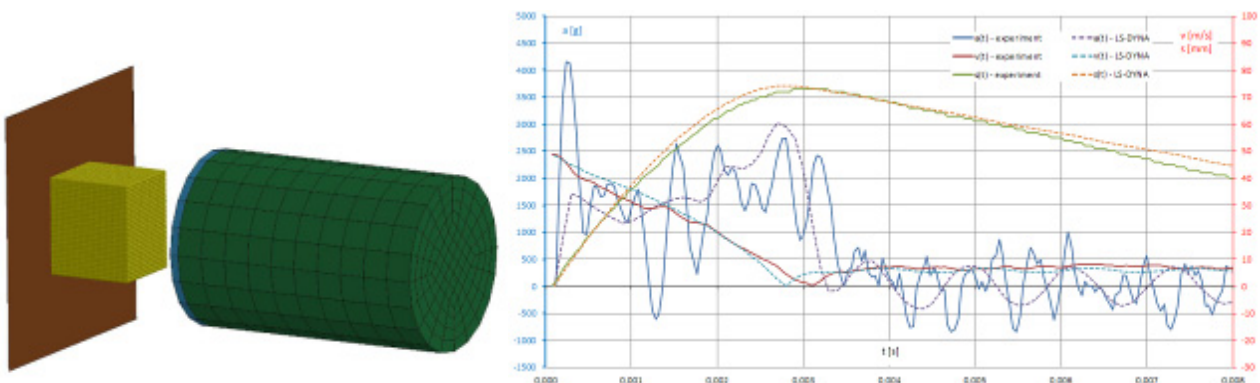


Figure 5-10: Comparison of experiment and numerical data for SR10 material



### High speed dynamic tests (scale 1)

The following step consisted of high speed tests at larger scale. As it had been proven to be successful, the same technique with the air cannon was used again. A scale one specimen was considered, featuring appropriate dimensions for the foam block and for the bullet representing the container (see Figure 5-11). Three different densities of the PU foam Puren were used for these tests. The demonstrated interest of PU foam, as well as the possible procurement of large blocks, were the main reasons for this choice.



Figure 5-11: Cannon and 5.5 kg bullet (top) – Impacted foam block (bottom)

As in previous step, a numerical rebuilding of tests was then performed with the LS-Dyna code. Again, a good comparison was obtained between the FEM model and the experiment data.

### Numerical Simulations

A scale one simulation was finally performed, including only the foam and the sample container, not the whole capsule. A sensitivity analysis showed a very limited influence of the foam initial velocity (zero, or same as the one of container).

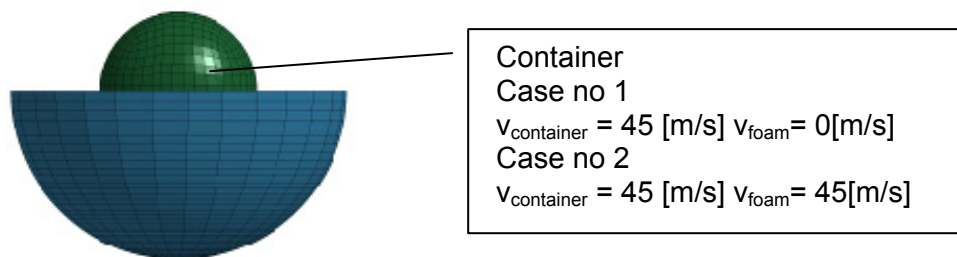


Figure 5-12: FEM model for scale 1 simulation



## Demonstrator

After final selection of materials for crushable structure, a technology demonstrator was made. It is made of Puren 145, and manufactured according to dimensions given by Demokritos in order to fit to the TPS demonstrator described in a former section. IoA made also a demonstrator of Payload which is an aluminum sphere. Both Crushable Structure and Payload Breadboards are shown in Figure 5-13 below.



Figure 5-13: Crushable and payload breadboard – for integration with TPS demonstrator by Demokritos

## Conclusion of activities on crushable materials

This activity on crushable materials results in several valuable outcomes, which can be summarized as follows:

- An efficient methodology has been elaborated, based on a two-step experimental approach
  - Static tests that provide strength behaviour and capability for energy absorption for the considered materials.
  - Impact tests using the air cannon technique.
- Numerical simulations of impact tests with LS-Dyna, using static tests results as inputs, give a good correlation between experimental and computed data
  - Validity has been demonstrated for PU foams, and should be further verified for other types of materials
  - It is possible numerically to simulate various geometries based only on static test results
- After setup pneumatic cannon test procedure turns out to be a very efficient methodology, which allows to perform 10 – 12 tests per day –
  - High speed camera and picture analysis software works perfectly with project application
  - A high mastery of the measurements is essential, because the use of pneumatic cannon for dynamic test gives important energy differences with small velocity variation
- Finally, the material identified as the most promising was selected for delivery of a representative breadboard to be integrated within the technological demonstrator.



## 6. WP 4: ABLATION - FIGHT MECHANICS COUPLING ASSESSMENT

### 6.1 IMPLEMENTATION AND ASSESSMENT OF COUPLED TOOL

High surface recession is expected on high-speed Earth entry capsule with impact on the aeroshape modification, the centre-of-gravity displacement and possibly on aerodynamic stability and the drag performances.

The main objective of this task was to assess the impact of massive ablation on aerodynamic performances and stability along the entry trajectory path. High TPS recession might occur during high-speed entries and it is necessary to identify which recession level could be tolerated with respect to capsule aerodynamic performances and stability requirements.

#### Astrium ST coupled tool

In order to address this topic, it is necessary to use an approach that couples aeroshape aerodynamic, trajectory and stability, aerothermal environment, TPS material thermal response and recession determination resulting in aeroshape modification. Such a coupled tool has been developed by Astrium ST : its main requirements and assumptions are discussed hereafter.

This tool has been developed following four main requirements.

- **Modularity:** this deals with the general architecture of the coupling tool. Basically the tool is constituted by two general entities: Functional Class Tools and Modules. A functional class tool is an interface between a generic task (Aerodynamics, Thermal response, Trajectory...) and a module attached to specific software chosen by the user. A functional class manages all the inputs/outputs needed for the functioning of all the modules in the coupling tool.
- **Robustness:** This requirement of robustness is particularly important for high speed entry where strong gradients (recession rate, temperature, mass loss...) can occur during the computation of a whole trajectory. This requirement has an impact on the choice of the module (software) employed inside a Functional Class.
- **Evolutionary Tool:** This is a basic but not to neglect requirement for scientific software. This is also an important requirement to keep the tool easily adaptable, also facilitated by its modular architecture.
- **12 CPU hours** is the target duration to perform a complete trajectory.

For the present study the coupling tool is constituted by 6 specific Functional classes associated with 6 modules, the main assumptions of which are sum up in the following table:

Trajectory tool	3 DoF mode
Aero-thermodynamics engineering tool	Aerodynamic coefficients, Convective and radiative heat flux, transition criteria...
Material response tool	Pyrolysis module: Arrhenius laws Ablation module: Chemical tables Boundary conditions: Convective + radiative heat fluxes Blockage effect: Only on convective heat flux $f(M_{\text{gas injected}}/M_{\text{air}}, T, P, \text{regime})$
Ablated Aeroshape Rebuilding Tool	This tool data processes the Material Response Tool output as recession and Mass loss per $m^2$ into ablated profile coordinates and global mass loss as input for MCI Tool and CFD Tool.
CFD Tool	- Inviscid - Gas at chemical equilibrium - Hypersonic/ supersonic regime from $2 < \text{Mach} < 42$
Mass Centering Inertia Tool	Outputs: updated mass table used for the next loop of the trajectory tool and the displacement of CoG due to shape and mass change. The initial position of the $X_{\text{CoG}}$ capsule is $-0.296m$ (26.9% of $L_{\text{ref}}$ )

Table 6-1: Functional classes and main assumptions of the corresponding modules



Another assumption is worth being mentioned: The drag coefficients on modified aeroshape employed to update the trajectory are determined by an additive correction of the Drag coefficients on the nominal aeroshape from the initial aerodynamic data base. This correction is determined on both ablated/ non ablated aeroshape thanks to the CFD tool.

This correction is applied on the hypersonic/supersonic domain from Mach 42 to 2 which corresponds to an altitude range from 71km to 30km. Neither transonic/subsonic correction nor rarefied aerodynamics has been done at present, which could be a relevant task for further enhancement.

The global functioning is described in the flow chart presented in Figure 6-1.

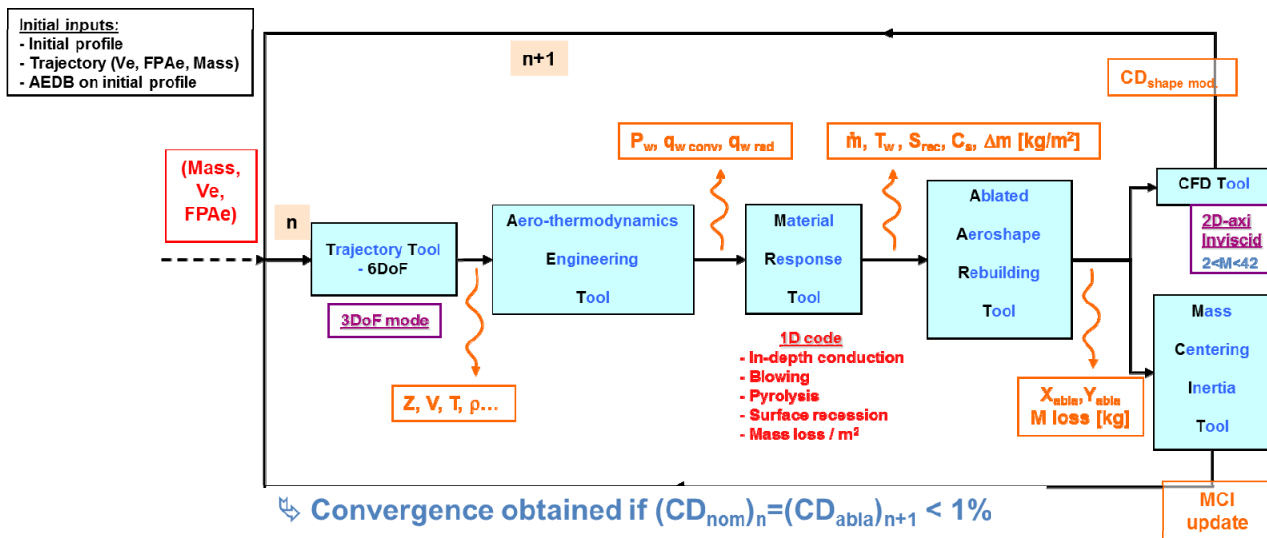


Figure 6-1: Flow chart of the coupling tool

**Preliminary coupling assessments**

The application case for identification of aeroshape modification / mass change coupling has been done on the ERC aeroshape (see Table 6-2) for two selected trajectories described here below (see Table 6-2).



Sphero-conical	capsule
Diameter	D =1100 mm
Half cone angle	45°
Nose radius	Rn = 275 mm (Rn / D = 0.25)
Shoulder radius	Rs =27.5 mm (Rs / D = 0.025)
Sref	0.95 m²

Table 6-2 – ERC shape and dimensions

	Traj. 1	Traj. 2
Entry Velocity at 120km	12.3km/s	12.3km/s
Flight path angle (FPAe)	-12.5°	-16.8°
Initial mass	66.7kg	66,7kg

Table 6-3 – Trajectory characteristics at entry



The observed impacts on trajectory parameters compared with no coupling case (nominal) for the two trajectories can be summarised as in Table 6-4.

Considering the model employed for the material response tool, the trajectory conditions and the nominal aeroshape, the aeroshape modification due to ablation in the high velocity domain is weak which can produce a low effect on trajectory but it has been found that on maximum heat flux trajectory the shape coupling has an effect of about 1km in the final range and therefore on the precision at impact. Due to aeroshape change the Center of Gravity of the heatshield moves backward of about 4-5mm which is also weak.

Parameters	Effects / nominal case	Maximum levels difference	% vs. nominal case	Criticality
Velocity	↔	50 ↔ 75m/s	~1%	Low
Mach	↔	0.15 ↔ 0.25	~1%	Low
Deceleration	↔	-0.5 ↔ 1g	1% ↔ 1.5%	Low
Dynamic pressure	↔	1.2 ↔ 1.7kPa	~3% ↔ 3.5%	Medium
Stagnation pressure	↔	2 ↔ 3kPa	~2.5% ↔ 4%	Medium
Heat Fluxes	↔	<100W/m <sup>2</sup>	~0%	Negligible
Heat Load	↔	1.5 ↔ 2.5MJ/m <sup>2</sup>	1% ↔ 2%	Medium
Range	↔	0.8 ↔ 1.4km	~0.3%	Medium

Table 6-4 – Coupling effect comparisons on trajectory parameters

The first objective of this preliminary work was successfully achieved, which was to develop the coupling tool, and to test its ability to reach the main initial requirements.

Potential further work is identified on a few points, in order to continue enhancing the methodology:

- Massive ablation due to higher level of entry velocity could produce more important aeroshape modification and therefore stronger impact on trajectory, precision, MCI ... Further evaluation on more demanding trajectories is therefore appropriate to assess this aspect.
- The aeroshape modification in Transsonic/Subsonic domain cannot be taken into account in this version. This should be a relevant improvement, for which the use of NS computations seems the best way. However, this would result in strong investment on mesh activities, with increase of CPU time and potential impact on robustness.

## 6.2 ENGINEERING MODELLING CORRECTION BY CFD (WP 4.3)

As the modules constituting the coupled tools are essentially engineering codes based on simplified correlations, one way of improvement is to refine these correlations, relying on results from detailed CFD analyses. This activity was undertaken within WP4.3, and a series of computations was carried out, addressing the following items:

- Mass blowing influence on convection and radiation (8 points B1 to B8, selected to get a good coverage of the entire trajectory, as illustrated on Figure 6-2),
- Aeroshape modification influence on aerodynamics and aerothermodynamics (6 points M1 to M6),
- Non-equilibrium radiation (12 points R1 to R12).

These items have been split into four different sub-tasks [11]. CIRA was in charge of flow-field computations while radiation was analysed by CNRS.

Unfortunately, not all results were satisfactory for these complex CFD analyses, and further consolidation would be necessary, which was not achievable within the resources of the project.



However, following recommendations about the different correlations can already be derived from the partial conclusions obtained so far.

- Aerodynamic coefficient
  - CFD computations show that current correlations are valid (to be consolidated for high velocities)
- Convective heat flux
  - Correlations used for coupling tool are kept by conservatism
  - No firm trend may be derived from current CFD computations, which require further consolidation
- Radiative heat flux
  - Correlation can be updated, as a reduction of shock stand-off distance on stagnation line is observed.
  - A subsequent reduction of level of radiative heat flux is thus anticipated.
  - This would require to be extended for a larger range of entry velocities.
  - Finally, the interest for actually fully coupled flowfield /radiation computations remains high.

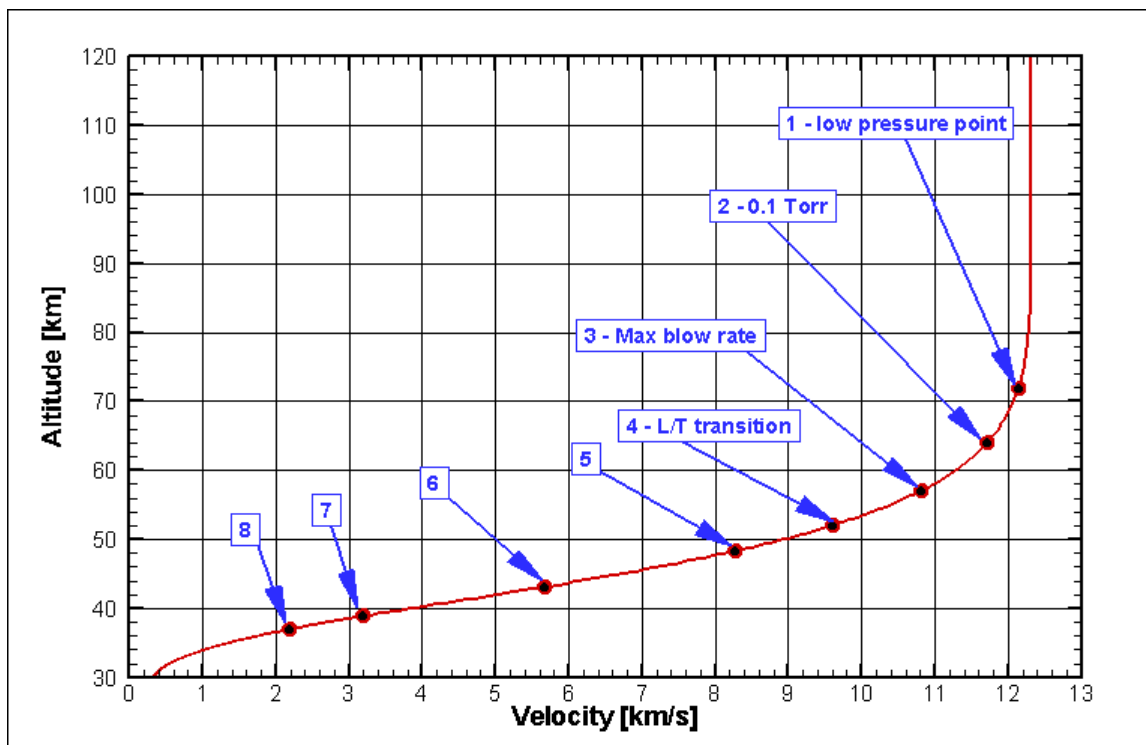


Figure 6-2: The 8 trajectory points considered for blowing assessment



### 6.3 EXPERIMENTAL ASSESSMENT OF RADIATING SPECIES AROUND ABLATING MATERIALS (WP4.4 - CNRS)

Products ablated from the protective shield of a superorbital velocity re-entering vehicle may react with the incoming air plasma flow, thus producing chemical species such as C, C<sub>2</sub>, C<sub>3</sub>, CN, CO, CO<sub>2</sub>, ... that can couple with those contained in the incoming air flowfield. These products may affect the absorption and emission properties of the boundary layer, thus potentially affecting the radiative heat flux to the surface of the superorbital velocity vehicle.

Thanks to remaining resources, it was proposed as additional work to complement the numerical simulations of WP4.3 by performing an experimental assessment of the feasibility of measuring these products in the 50 kW plasma torch facility of EM2C. The following tasks have been successfully completed:

- Installation of the plasma torch facility shown in Figure 6-3
- Implementation of the optical emission spectroscopy system depicted in Figure 6-4 (Nov 2011-Sept 2012)
  - Two surface T° measurements, using one single color and one two-color pyrometers
  - One low resolution broadband Spectrometer OceanOptics USB2000+
  - One high resolution spectrometer Acton SpectraPro 2750
- Design and building of an ablative layer holder (March-June 2012) designed to support a cylindrical ablator coupon (ASTERM, CBCF, ...) in the plasma stream (see Figure 6-5)
  - Water-cooled sting holds a 5 mm thick, 40 mm diameter copper disk
- First tests of plasma torch facility in air and adjustments (Sept-Nov 2012)
- Characterization of torch operating conditions in air: spectroscopic measurements of plasma temperature and calorimetric measurements of specific heat. Tests of ablator holder system (Dec. 2012 – Jan 2013)
- Experiments with ASTERM ablating material exposed to air plasma: measurements of ablator surface temperature, of heat flux to the ablator surface, of low and high resolution emission spectra. Analysis of results.
- Material temperature and species concentration profiles were measured in the boundary layer, showing spallated particles, sodium emission, plasma recombination.



Figure 6-3: plasma torch facility

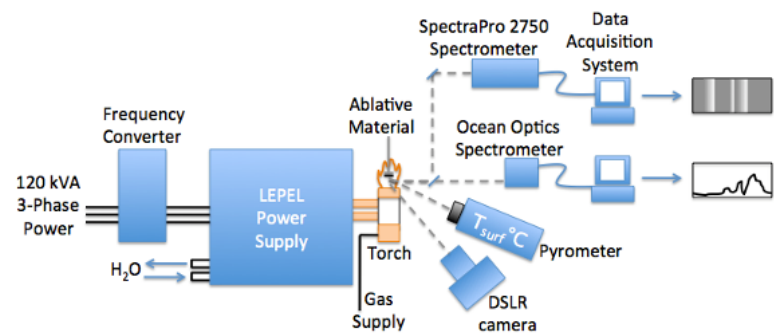


Figure 6-4: Optical emission spectroscopy system

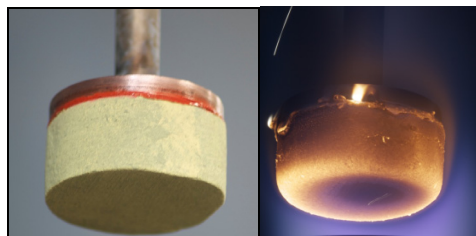


Figure 6-5: Ablative layer

The facility is now fully operational and ready for more testing and experimental research work such as:

- Investigation of material behaviour under test conditions with higher power and heat flux
- Search for more species (C, C<sub>2</sub>, C<sub>3</sub>)



## 7. WP5: GAS-SURFACE INTERACTION MODELLING

### 7.1 AN EXPERIMENT TO SIMULATE THE COUPLING BETWEEN ABLATION AND PYROLYSIS PRODUCTS

It is well known that during re-entry, and in particular for high speed re-entry, the TPS surface degradation results in rough surfaces that enhance dramatically the turbulent heating. In case of high gas surface blowing due to massive ablation, blowing might encompass roughness-induced overheating. The general objective of the present work package is to carry out an experimental investigation of the coupling between surface roughness and blowing due to ablation and pyrolysis products and to identify possible margins saving.

The ONERA Meudon center R2Ch wind tunnel was used for the experiments. R2Ch wind tunnel is a blow-down facility (test duration between 15 and 30 seconds) equipped with its Mach 5 nozzle for this test campaign.

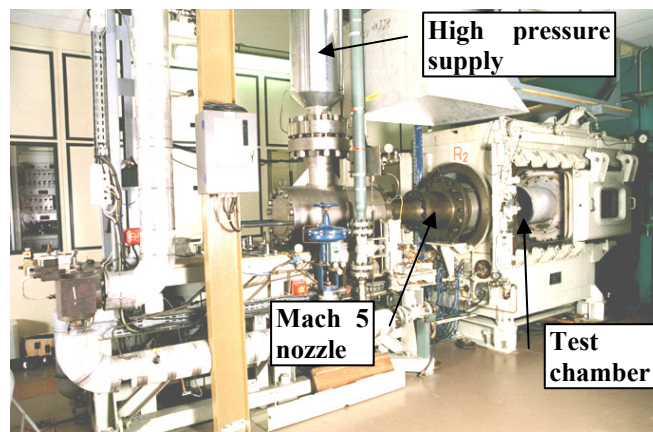


Figure 7-1: ONERA R2Ch facility

A flat plate model with a sharp leading edge was used for those experiments at  $0^\circ$  incidence. An exploded view of the set-up in the R2Ch test-chamber is shown in Figure 7-2, the flow direction being from the nozzle on the left to the right. The model was equipped with two inserts: one made out of steel (isotan) and one made out of ceramics represented in green on Figure 7-2. Furthermore, in order to reproduce the real effect of an ablated wall, the model was pressurized, and pressurized air was blown through the porous wall from a tank located under the insert.

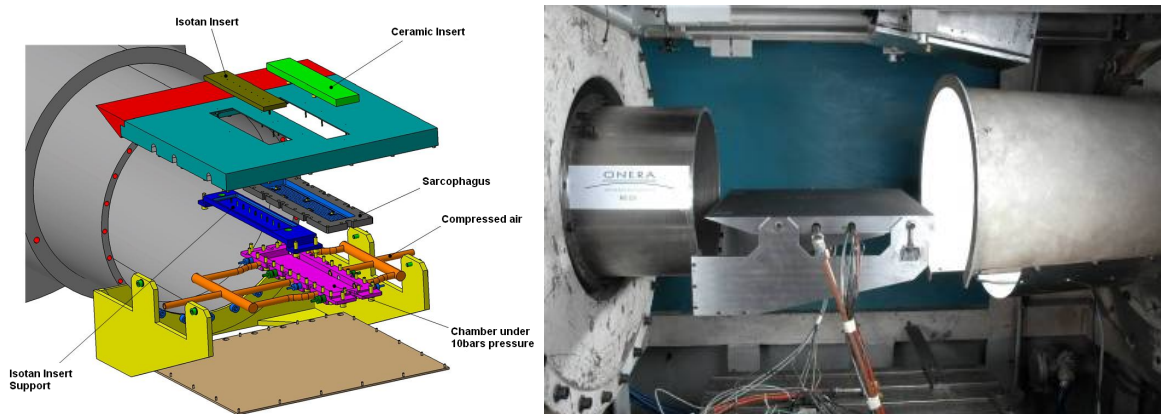


Figure 7-2: Exploded view (left) of the experimental set-up in the R2Ch test-chamber (right)



It has been chosen to reproduce an academic configuration (flat plate with regular roughness) in order to have the possibility to perform calculation. Indeed irregular roughness – as those obtained in reality during a reentry flight - could not easily being taken into account by a model. So it was decided to reproduce a regular pattern constituted by pyramidal roughness.

It was also required to use a material which simulates the deterioration of the wall surface state and the blowing effects. The wall in the experimental device was thus made out of porous rough ceramics in order to blow through the wall and hence to simulate the blowing due to ablation in reality.

Two porous ceramic inserts (one with and one without roughness) were manufactured by the firm CTI in Salindres in the south of France. The main features of such insert are a porosity of 48 %, and a roughness distribution made of regular truncated pyramids joined in alternate rows as shown in Figure 7-3.

The final insert was obtained after several uneasy iterations, and a detailed inspection enabled to determine its key parameters: the truncated pyramid height is  $176 \pm 34 \mu\text{m}$ , with a base of  $550 \mu\text{m}$ . Its overall dimension was also finally reduced from  $220 \times 40 \text{ mm}$  to  $100 \times 400 \text{ mm}$ , in order to limit mechanical efforts during the pressurised tests.

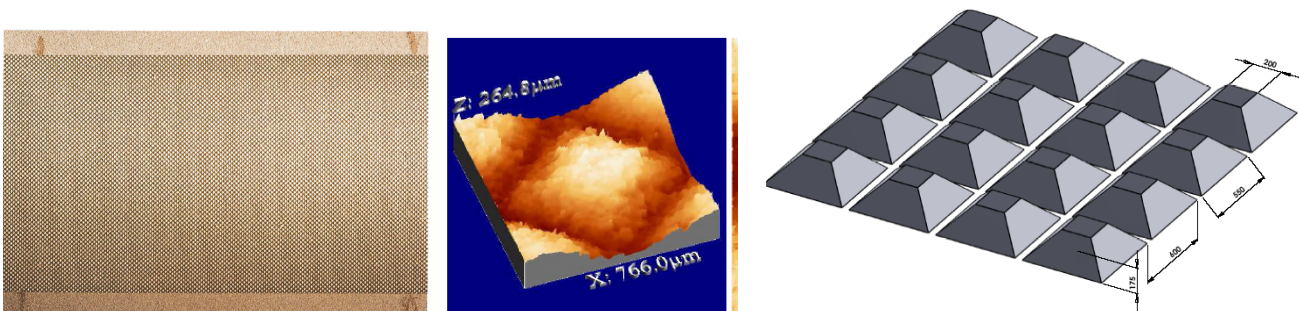


Figure 7-3: Photograph of pyramid distribution on the insert (left) – microphotograph of the surface (centre) – pattern used for modelling (right)

During the tests, Schlieren photographs of the flow are made, as well as heat flux measurements using infrared thermography technique. Successive thermograms are recorded at a frequency of 50 Hz and, for a known local heat capacity of the wall, the analysis of successive thermograms yields the heat flux on the investigated surface. Two parallel measurements are performed on the ceramic insert and on the reference Isotan insert located nearby. In addition, four thermocouples are implemented at the wall of the Isotan insert in order to check the infrared results.



Figure 7-4 – Schlieren photograph during one of the runs



## 7.2 EXPERIMENTAL RESULTS

Thirty-one documented runs (see Table 7-1) were performed in the hypersonic R2Ch wind tunnel for various conditions

- porous and rough wall
- with and without blowing : The mass flow rate level was determined in order to have a simulation in agreement with the reality along a classical re-entry trajectory. Tests were also run with an intermediate value corresponding approximately to the half of the highest mass flow rate.
- different stagnation pressures from  $p_{st} = 7 \cdot 10^{**5}$  Pa to  $p_{st} = 50 \cdot 10^{**5}$  Pa, which corresponds to unit Reynolds number from  $Re_L = 5.95 \cdot 10^{**6}$  to  $Re_L = 42.5 \cdot 10^{**6}$  with  $T_{st} = 650$  K

A few tests were also duplicated at the beginning in order to demonstrate the good repeatability of the tests conditions.

surface	Mass flow [kg/m²/s]	Stagnation pressure [Bar]		
		7	28	50
Smooth	0	3757 NT	-	3756 NT
		3764 NT		3763 NT
		3778 NT - BL		3759 NT - BL
	0.6	3780 TT	-	3774 NT - BL
		3779 TT - BL		3782 TT
		3772 NT		3775 NT - BL
1.12	3781 TT	3768 NT	3807 TT	
	3770 NT		3767 NT	
	3784 TT		3787 TT	
rough	0	3790 TT	-	3791 TT
		3802 NT		3792 TT
		3804 TT BL		
	0.66	3798 TT	-	3794 TT
		3799 TT		
		3803 NT		
1.15	3805 TT BL	-	3800 TT	

**Table 7-1 : Synthesis of R2ch runs**

*NT: natural transition TT: tripped transition BL: Boundary layer measurements*

The heat-fluxes have been deduced from the evolution of temperature – detected by infrared thermography - during the first seconds of the run. These heat-fluxes have been corrected by considering the variation of pressure during the run. The Stanton numbers have been deduced from these values by the following formula:

$$St = \Phi / \rho_{inf} U_{inf} C_p (T_{st} - T_w)$$

where  $\Phi$  is the heat-flux in W/m²,  $\rho_{inf}$  and  $U_{inf}$  are respectively the density and the velocity delivered by the nozzle,  $T_{st}$  the stagnation temperature and  $T_w$  the wall temperature and  $C_p$  is the calorific coefficient at constant pressure equal to 1003 J/kg/K.

The Figure 7-5 presents the evolution of the Stanton number along the X-axis for two different runs. The first abscissa  $X = 140$  mm corresponds to the position of the two inserts at 140 mm from the leading edge. The green curve is relative to the Stanton numbers deduced from the infrared results obtained onto the ceramics insert. The red curve is relative to the Stanton numbers obtained onto the isotan insert. These last results are in excellent agreement with the Stanton numbers – represented with the blue points - deduced from the thermocouples implemented inside the isotan inserts. The eventual difference between the two curves has then to be corrected with an adjustment of surface emissivity and temperature of the ceramic insert.



At low pressure ( $p_{st} = 7 \times 10^5 \text{ Pa}$  – left), an increase of the heat flux is observed which is the sign of the transition of regime from laminar to turbulent. At high pressure, ( $p_{st} = 50 \times 10^5 \text{ Pa}$  – right), the flow is fully turbulent on the entire insert.

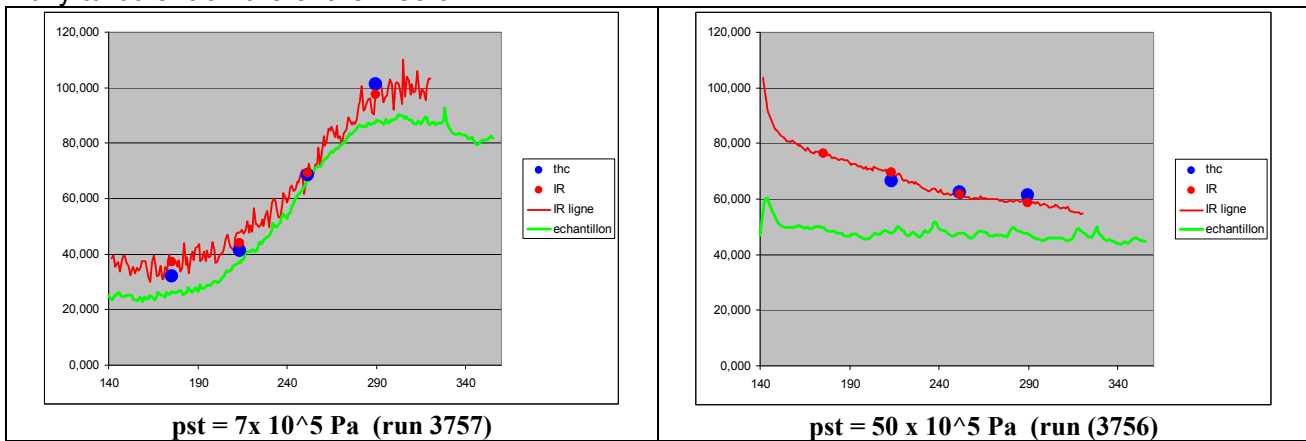


Figure 7-5 – Evolution of the Stanton number along the X-axis

Comparison between the different runs enables the identification of typical key behaviours.

- Smooth wall with blowing: Figure 7-6 shows the decrease of Stanton number along the ceramic insert with a smooth wall, when blowing is increased. The observed reduction is about 55-60% for the intermediate mass blow rate ( $0,6 \text{ kg/m}^2/\text{s}$ ) and 70-80% for the maximum mass rate which is rather important.
- Rough wall without blowing: The experiment over rough surface without blowing gives an unexpected decrease of Stanton number whereas an increase is expected (see Figure 7-7). Presently no satisfactory explanation is available to understand this point.

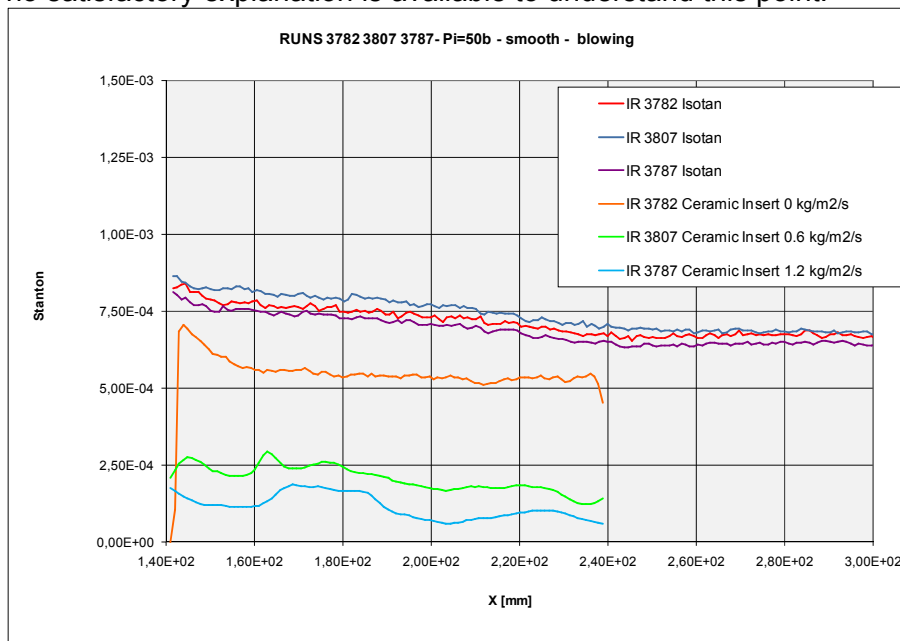


Figure 7-6 – Effect of blowing on Stanton number at 50bar



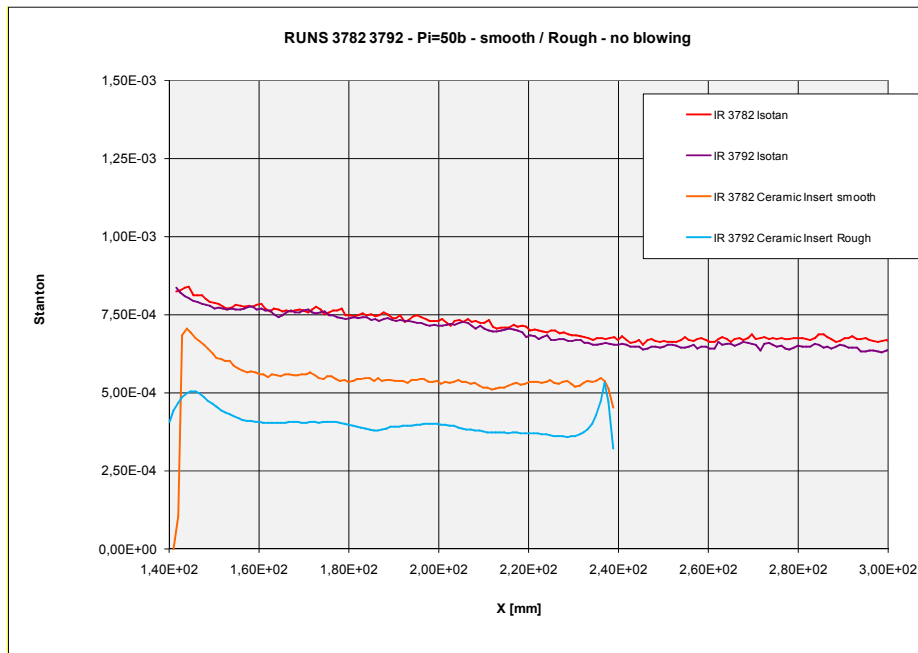


Figure 7-7: Stanton number comparisons for smooth and rough cases without blowing



## 7.3 GAS-SURFACE INTERACTION MODELLING

### Review of surface roughness and blowing influence (WP 5.1)

A review of surface roughness and blowing influence on aerothermodynamics has been performed by Astrium-ST and MSU, with a complementary support by Onera through a review concerning roughness effects. This work was completed by a review of blowing effects by MSU, which was in particular constructively extended based on research works performed in Russia.

Thanks to these elements, MSU worked on a model description and concluded that it is possible to take blowing effects into account by changing a velocity profile from a logarithmic one. After scientific discussion with Onera experts, the idea has been polished to obtain a robust approach.

The selected model was implemented by Onera in a boundary layer solver and by CFS in a Navier-Stokes code (NSMB).

### Boundary layer calculations (WP 5.2.3)

This part of the work consisted in a numerical rebuilding of the experiments carried out in WP5.2. It was performed by ONERA using a Boundary Layer code.

Among all the documented runs, some were disregarded either because they correspond to a total pressure of  $28 \times 10^5$  Pa for which no way to estimate where the transition takes place is available or to a total pressure of  $7 \times 10^5$  Pa and are highly polluted by transition effects. Finally, seventeen runs were computed. With various hypotheses on wall temperature and transition location and various turbulence models with some variants, this led to a total of 244 different computations, which brings into evidence the interest of a boundary layer code to be able to investigate so many cases at a reasonable cost.

The analysis of the model predictions for the runs over the smooth surface pointed out the importance of the transition on the flow structure. Without tripping, the transition takes place close to the inserts at the highest total pressure and ends just at the beginning of the insert. At the lowest total pressure, the transition process extends all over the insert. With tripping, the transition takes place some distance after the rough trip for the lowest total pressure and still affects the flow on the insert. This led to favour the highest total pressure cases to investigate turbulent flow modelling.

The investigation of the smooth wall runs also evidenced two problems. The Stanton number measurements on the Isotan insert could quite easily be reproduced, while it was necessary to significantly increase the wall temperature to reproduce those on the ceramic insert,.

The small blowing mass flow run is rather well predicted by all models. The strong blowing mass flow run points out the need for a blowing correction in the Spalart and Allmaras model. Cebeci's correction for wall blowing seems to be too strong.

The investigation of runs over rough surfaces without blowing evidences a sorting between roughness models. Krogstadt's, Boeing's and Wilcox' corrections predict stronger roughness effects than Rotta's, Blanchard's and ONERA's ones. The puzzling point is that there were not such differences between models in low speed test cases, for the same range of reduced roughness heights for much closer predictions between Boeing and ONERA corrections. This is suspected to be due to the coupling between the way the roughness correction acts and the density gradients in the wall region.

The prediction of runs over rough surface is very problematic as experiments give an unexpected decrease of the Stanton number on rough surfaces while models predict an increase, as usual. The fact that the roughness elements are porous, while models were developed and validated for solid roughness elements, does not seem to be enough to explain this discrepancy.

At last, investigation of runs coupling wall roughness and blowing brought the unexpected result that the roughness model ranking obtained without wall blowing is completely reversed in presence of wall blowing. An open question is whether or not model should account for near-wall turbulence enhancement by both blowing and roughness effects. Unfortunately, these runs did not really allow selecting the best model.



## 7.4 CFD MODELLING (WP5.3 - CFS)

### CFD Code Adaptation (WP5.3.1)

The NSMB CFD code used in this project was extended with rough surface turbulence models. The well-known 1-equation turbulence model of Spalart-Allmaras was extended to rough surfaces using the method proposed by Bertrand Aupoix of ONERA. In addition, the  $k-\omega$  family of turbulence models was extended to rough surfaces using the method proposed by Wilcox, and using the method proposed by Knopp (which is based on the work of Bertrand Aupoix for the Spalart Allmaras turbulence model). The  $k-\omega$  family of models was also extended for blowing using the method proposed by Wilcox. Validation simulations were carried out for two rough surface experiments, and for one experiment with blowing.

### Wind Tunnel Test reconstruction (WP5.3.2)

The objective of this task was the CFD rebuilding of the wind tunnel experiments carried out in WP5.2. CFD simulations were performed using the adapted code as described above.

A reduced selection of six runs was considered for Navier Stokes CFD calculations, as reminded in Table 7-2. The results of the CFD calculations were compared with the experimental results and with results of Euler-boundary layer computations made at ONERA. The results of the Navier Stokes calculations show a good agreement with the results of the Euler-boundary layer simulations, and a reasonable agreement with the experimental results.

Case	1	2	3	4	5	6
Run#	3782	3807	3787	3792	3794	3800
Blowing rate	0	2.6 g/s (~0.6 kg/m <sup>2</sup> /s)	4.8 g/s (~1.2 kg/m <sup>2</sup> /s)	0	2.63 g/s (~0.6 kg/m <sup>2</sup> /s)	4.6g/s (~1.2 kg/m <sup>2</sup> /s)
Roughness	Smooth	Smooth	Smooth	176µm	176µm	176µm

Table 7-2 : Experiments selected for Navier Stokes CFD simulations

As an example, Figure 7-8 shows typical comparisons of the Stanton number for the case with a smooth insert with blowing at 0.6 kg/m<sup>2</sup>/s (Case 2 – Run 3807). Until the start of the Ceramic insert (at  $x=0.138\text{m}$ ) the computed Stanton number is very close to the results for the case without blowing, as expected. On the Ceramic insert the computed Stanton number using the Spalart Allmaras turbulence model is slightly higher than the one computed using the  $k-\omega$  Menter Shear Stress model. For the Spalart Allmaras turbulence model there is also a good agreement between the Navier Stokes and boundary layer calculations. Both Navier-Stokes and boundary layer calculations slightly underestimate the measured Stanton number in the middle of the ceramic insert.

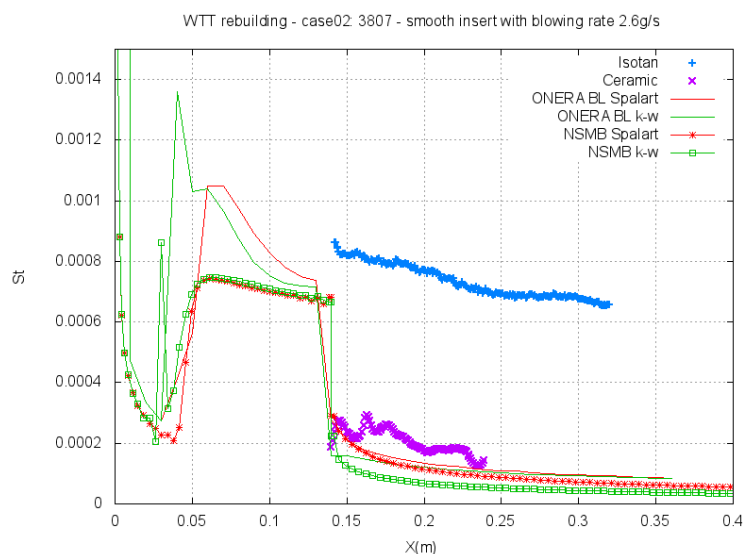


Figure 7-8 – Evolution of the Stanton: smooth wall , blowing rate 0.6 kg/m<sup>2</sup>/s



### **Earth Re-entry vehicle computations (WP5.3.3)**

This last part of the activity consisted of an application to the entire capsule, also including most of the improvements implemented based on previous tasks. The grid for the Re-entry vehicle was based on the one used by CIRA within WP4. It was modified at CFS Engineering to permit the use of shock adaptation technique to improve the quality of the solution. For three selected trajectory points, two different roughness heights and two different turbulence models were considered. The influence of the ablation of the TPS material was simulated through the injection of mass (blowing) at the solid wall. For each trajectory point the mass flow rate was provided by Astrium at different locations along the capsule geometry. The NSMB code was modified to permit the reading of the mass flow rate data files and to interpolate the prescribed values on the CFD mesh. The change in geometry due to the ablating TPS material was not taken into account in these CFD simulations.

After discussion of the initial results it was decided to complete these calculations by sensitivity studies for one of the considered conditions. Additional calculations were made for a smooth wall, for a wall without mass injection, for a laminar flow and using the k- $\omega$  Wilcox turbulence model using different roughness models.

## **7.5 SUMMARY STATUS FOR WP5**

The main outcomes of the activities carried out within this WP5 “Gas-surface interactions modelling” are summarized hereafter.

After a preparation work requiring several adjustments, the characteristics of the ground experiment were appropriately fixed, and a series of wind tunnel tests was then carried out.

- A good repeatability of the run has been evidenced,
- Lot of valuable experimental data have been acquired.

After implementation of both roughness and blowing effects in different solvers, computations and comparison with the experimental data were undertaken. A good agreement between the different solvers was observed: Boundary Layer Euler solver (ONERA) and NSMB - Navier-Stokes Multi-Blocks (CFS). The main conclusions of these comparisons are as follows:

- Wall blowing : Correct agreement of CFD simulations
  - Small blowing : the important observed heat flux decrease is well predicted by all models
  - Strong blowing mass flow case evidences the lack of a blowing correction for the Spalart and Allmaras mode
- Wall roughness : a key issue is highlighted
  - Models predict heat flux increase, while experiment show heat flux decrease. This remains unexplained (porosity of the insert, repeat tests with a much higher roughness?)
- Wall roughness + blowing cases are more complicated to simulate
  - Models which cannot account for wall blowing (Spalart, k- $\omega$ ) predict too low levels
- No obvious best choice between Spalart and k- $\omega$  models



## 8. WP6: MANAGEMENT, DISSEMINATION AND EXPLOITATION

To disseminate the outcomes of the project, a website for the project was created ([www.rastas-spear.eu](http://www.rastas-spear.eu)) and the project was presented at 8 relevant events (Table 8-1).

Event	Content	Date	Venue
3 <sup>rd</sup> International Atmospheric Re-entry Association days <a href="http://www.avantage-aquitaine.com/conferences/ARA2011/">http://www.avantage-aquitaine.com/conferences/ARA2011/</a>	<ul style="list-style-type: none"> <li>Oral presentation + paper : J-M. Bouilly et al, RASTAS SPEAR: Radiation-Shapes-Thermal Protection Investigations for High Speed Earth Re-entry</li> </ul>	2011, May 2-4	Arcachon, France
Let's embrace space - FP7 space conference 2011	<ul style="list-style-type: none"> <li>Oral presentation : G. Vekinis</li> </ul>	2011, May 12-13	Budapest, Hungary
8 <sup>th</sup> International Planetary Probe Workshop (IPPW 8) <a href="http://www.planetaryprobe.org/">http://www.planetaryprobe.org/</a>	<ul style="list-style-type: none"> <li>Poster presentation : J-M. Bouilly et al, RASTAS SPEAR: <u>Radiation-Shapes-Thermal Protection Investigations</u> for High Speed Earth Re-entry</li> </ul>	2011, June 6-10	Portsmouth, Virginia, USA
9 <sup>th</sup> International Planetary Probe Workshop (IPPW 9) <a href="http://www.planetaryprobe.eu/">http://www.planetaryprobe.eu/</a>	<ul style="list-style-type: none"> <li>1 Oral presentation: J-M. Bouilly et al, RASTAS SPEAR: Radiation-Shapes-Thermal Protection Investigations for High Speed Earth Re-entry</li> <li>1 Poster : Mechanical behaviour of adhesively bonded ASTERM ablative TPS after Plasma-jet testing G. Vekinis and A. Marinou NCSR Demokritos, Greece</li> </ul>	2012, June 18-22	Toulouse, France
18th AIAA/3AF International Space Planes and Hypersonic Systems and Technologies Conference	<ul style="list-style-type: none"> <li>Oral presentation :G. Pezzella P. Catalano (CIRA), A. Bourgoing (Astrium) - Computational Flowfield Analysis of a Sample Return Capsule</li> </ul>	24–28 September 2012	Tours, France
63 <sup>rd</sup> International Astronautical congress	<ul style="list-style-type: none"> <li>Poster presentation : A. Pisseloup et al, RASTAS SPEAR: Radiation-Shapes-Thermal Protection Investigations for High Speed Earth Re-entry</li> </ul>	2012, Oct 1-5	Naples, Italy
Gordon Research Conference : Atmospheric Reentry Physics <a href="http://www.grc.org/programs.aspx?year=2013&amp;program=atmosentry">http://www.grc.org/programs.aspx?year=2013&amp;program=atmosentry</a>	<ul style="list-style-type: none"> <li>Poster presentation: D. Kuznetsova, M. Gritsevich, V. Vinnikov (MSU) - Modeling the turbulent boundary layer with account for surface roughness and blowing</li> </ul>	February 3-8, 2013	Ventura (CA), USA
7 <sup>th</sup> European Workshop on TPS & Hot Structures <a href="http://www.congrexprojects.com/13c06/programme">http://www.congrexprojects.com/13c06/programme</a>	<ul style="list-style-type: none"> <li>Oral presentation : RASTAS SPEAR : Radiation-Shapes-Thermal Protection Investigations for High Speed Earth Re-entry – J-M. Bouilly, Astrium Space Transportation</li> <li>Oral presentation : “Gas-Surface Interactions modelling” - B.Chanetz, Onera</li> <li>Oral presentation : “High Speed Entry Ablation-Flight Mechanics Coupling Effects” A. Bourgoing, Astrium Space Transportation</li> </ul>	2013, April 8-10	Noordwijk (NL)



Event	Content	Date	Venue
	<ul style="list-style-type: none"> <li>Oral presentation : "Overview of the TPS Activities within the RASTAS SPEAR Project" G. Vekinis, NCSR Demokritos</li> </ul>		
	<ul style="list-style-type: none"> <li>Oral presentation : "Characterization of a 50 kW Inductively Coupled Plasma Torch for use in Testing of Ablative Materials" - M. MacDonald, Ecole Centrale</li> </ul>		

Table 8-1: presentations of the project



## 9. CONCLUSION

Rastas Spear was a typical R&D project, carried out thanks to the funding of European Community Framework Programme n°7 (FP7).

A well-defined framework was applied for the study, with a focus on a passive Earth Return Capsule. The project was completed in April 2013, with a successful achievement of overall project objectives, in particular.

- Increase TRL for key technologies such as crushable materials, or joints for thermal protection material,
- A relevant state of art of ground testing facilities for simulation of high speed entry was done, with a proposed concept for high enthalpy expansion tube, recognized as a currently missing facility.
- Development of suitable facilities, such as the air cannon for high speed testing of crushable materials, the plasma torch for investigation of coupled ablation-radiation phenomena, the rough and porous insert to experimentally address the Gas-Surface Interaction issues,
- Establishment of methodologies and tools, such as testing strategy proposed for super-orbital reentry, coupled tool developed for analysis of capsule entry, enhanced thermochemical models and turbulence models accounting for blowing and roughness to be included in CFD codes.

However, a few points show that further enhancement is still required, such as CFD modeling of complex coupled phenomena, and detailed understanding of combined influence of blowing and roughness on aerothermodynamic environment.

The outcomes of this project can be considered as a highly valuable step towards an actual flight mission, and especially for the following target missions currently under investigation at ESA: MarcoPolo-R, Phootprint, MSR...

